



A computational study of possible mechanisms of singlet oxygen generation in miniSOG photoactive protein

Goran Giudetti, Anastasia R. Blinova, Bella L. Grigorenko & Anna I. Krylov


To cite this article: Goran Giudetti, Anastasia R. Blinova, Bella L. Grigorenko & Anna I. Krylov (2026) A computational study of possible mechanisms of singlet oxygen generation in miniSOG photoactive protein, Molecular Physics, 124:3-4, e2396548, DOI: [10.1080/00268976.2024.2396548](https://doi.org/10.1080/00268976.2024.2396548)

To link to this article: <https://doi.org/10.1080/00268976.2024.2396548>

 View supplementary material 

 Published online: 05 Sep 2024.

 Submit your article to this journal 

 Article views: 114

 View related articles 

 View Crossmark data 

 Citing articles: 2 View citing articles 

A computational study of possible mechanisms of singlet oxygen generation in miniSOG photoactive protein

Goran Giudetti ^a, Anastasia R. Blinova^b, Bella L. Grigorenko ^b and Anna I. Krylov ^a

^aDepartment of Chemistry, University of Southern California, Los Angeles, CA, USA; ^bDepartment of Chemistry, Lomonosov Moscow State University, Moscow, Russia

ABSTRACT

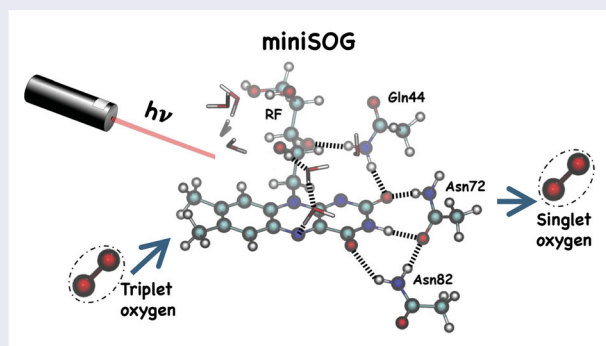
We report high-level electronic structure calculations of electronic states in the miniSOG (for mini Singlet Oxygen Generator) photoactive protein designed to produce singlet oxygen upon light exposure. We consider a model system with a riboflavin (RF) chromophore. To better understand the photosensitisation process, we compute relevant electronic states of the combined oxygen-chromophore system and their couplings. The calculations suggest that singlet oxygen can be produced both by intersystem crossing, via a triplet state of the $\text{RF}(T_1) \times \text{O}_2(^3\Sigma_g^-)$ character as well as by triplet excitation energy transfer via a singlet state of the same character. The calculations also suggest a pathway for the production of the triplet state of the chromophore via internal conversion facilitated by oxygen. Our results provide concrete support to previously hypothesised scenarios.

ARTICLE HISTORY

Received 17 June 2024
Accepted 19 August 2024

KEYWORDS

Photosensitisation;
spin-orbit interaction;
photoactive proteins; singlet
oxygen



1. Introduction


Genetically encodable photoactive proteins are used in a variety of applications [1,2]. Of particular interest are photoactive systems that can generate reactive oxygen species (ROS) upon exposure to light. The interest in such systems stems from their uses in electronic microscopy [3], photodynamic therapy [4] and chromophore-assisted laser cell inactivation [5]. One such protein is miniSOG (for mini Singlet Oxygen Generator) – a small (106 amino acid residues) flavin-containing protein capable of generating ROS when stimulated by blue light [6]. miniSOG is the first flavin-binding protein developed specifically as a genetically encodable light-induced source of singlet oxygen.

The chromophore in miniSOG is flavin mononucleotide (FMN), however, variants with a riboflavin (RF)

cofactor have also been investigated [7,8]. Figure 1 shows the miniSOG structure as well as structures of the FMN and RF chromophores.

Interestingly, the quantum yield of singlet oxygen production in miniSOG is much smaller than that in free FMN – i.e. 0.03 versus 0.51 (see, for example, Ref. [7]), which has been attributed to the effective quenching of the FMN's triplet state by the protein via electron transfer [7,9,10]. This undesirable quenching by the protein has also been deemed responsible for producing other types of ROS, such as peroxide [9], which is undesirable for applications. Several studies reported modifications of miniSOG aiming to increase the quantum yield of singlet oxygen production [9,11]. For example, by mutating one residue forming a hydrogen bond with FMN, the quantum yield of $\text{O}_2(^1\Delta_g)$ was

CONTACT Anna I. Krylov  krylov@usc.edu  Department of Chemistry, University of Southern California, Los Angeles, CA 90089, USA

 Supplemental data for this article can be accessed online at <http://dx.doi.org/10.1080/00268976.2024.2396548>.

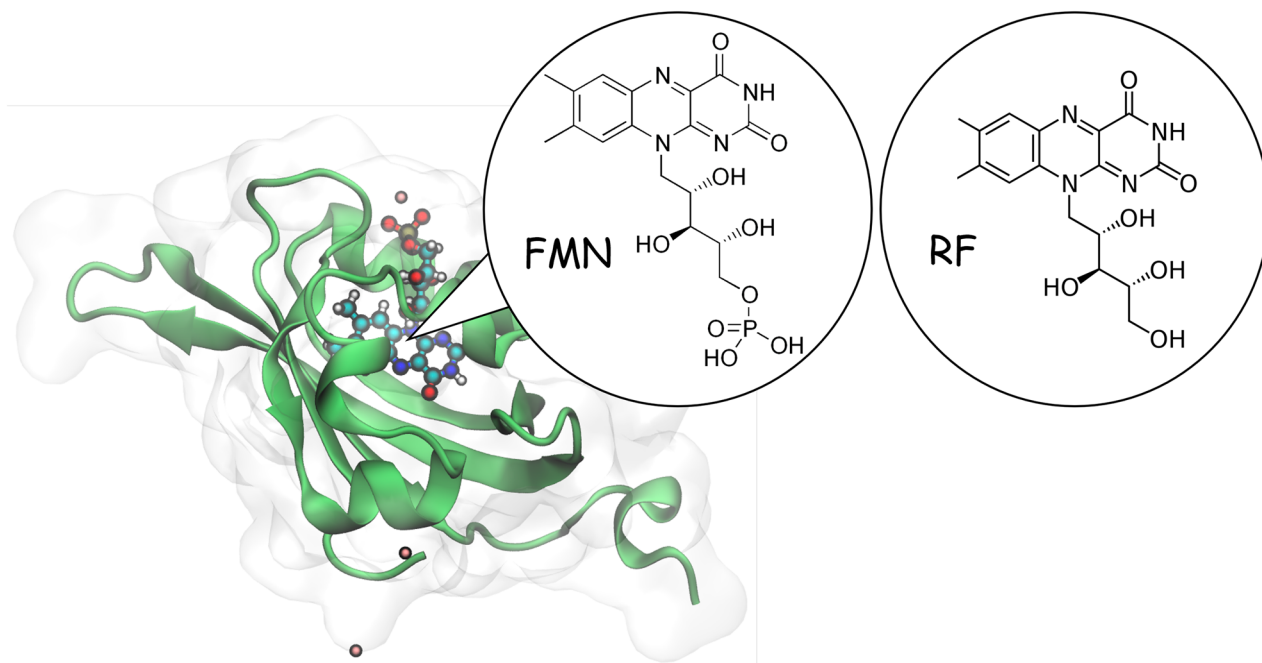


Figure 1. miniSOG protein. Flavin mononucleotide (FMN) and riboflavin (RF) cofactors are shown in the inserts.

increased up to ~ 0.2 in SOPP (singlet oxygen producing protein) [9,11].

It was also discovered that prolonged intense irradiation of miniSOG leads to an increase of singlet oxygen production [12]. The mechanism for this photoactivation involves photodegradation of FMN to lumichrome (LC), which increases chromophore's accessibility to oxygen [7] thus making oxygen quenching more effective than protein quenching of the triplet chromophore. This mechanistic interpretation of the structural data [7] is consistent with observations that the yield of singlet oxygen increases in both miniSOG and SOPP at elevated temperatures [10] due to protein's breathing motions favourable for oxygen diffusion.

The photodegradation phenomenon has been investigated in dozens of studies, which considered both free flavins [13–24] and flavin-containing proteins [25,26], however, the exact details of the mechanism have not yet been fully elucidated. The mechanism of photosensitisation in miniSOG is also not fully understood. Detailed molecular-level understanding of these processes is essential for the successful rational design of future miniSOG and SOPP variants aiming to improve the quantum yield of singlet oxygen production and the spectral properties of the protein.

Questions about the mechanism involve identification of electronic states involved in photosensitisation and photoconversion [27–30]. This requires calculations of singlet and triplet states as well as relevant electronic

couplings. In addition, characterisation of the effect of the protein environment on these quantities is important, as it is known that they strongly depend on the polarity of the environment [31–33].

Many computational studies investigated spin-orbit couplings (SOCs) in flavin proteins and flavin-like chromophores. For example, SOC calculations have been carried out to elucidate the reaction between FMN and neighbouring cysteine in LOV domains [34], to estimate the influence of the protein environment on the excited states of flavin [35], to describe the reverse cycle $\text{FADH}_2 \rightarrow \text{FAD}$, connected with the reduction of O_2 to H_2O_2 in glucose oxidase [36], to design fluorinated flavin derivatives with desired spectral properties [37], and so on.

The production of singlet oxygen [38] by photosensitisation, a transfer of electronic excitation from an electronically excited donor to a ground-state acceptor, occurs in many systems. This process is responsible for the ability of oxygen to effectively quench both fluorescence (i.e. singlet excited states) and phosphorescence (i.e. triplet excited states). Unlike Förster energy transfer [39], which involves transfer of dipole-allowed excitations and can happen between distant moieties, the transfer of spin-forbidden electronic excitations (triplet excitons via Dexter energy transfer) can only occur when the donor and acceptor are in close proximity [40]. Hence, the accessibility of the chromophores to dissolved oxygen is the key factor determining the efficiency of singlet oxygen generation.

The nature of electronic couplings responsible for singlet oxygen production and quenching of singlet and triplet excited states by oxygen has been extensively debated [38,41–43]. Despite the limited computational power, earlier theoretical works have developed insightful explanations of this process as well as related phenomena (e.g. ignition of slow fluorescence, singlet–triplet annihilation, collision-enhanced radiative transitions in oxygen, etc.) [42–47], which we can now confirm by high-level calculations. The two main scenarios of singlet oxygen production include intersystem crossing (ISC), facilitated by SOCs, and internal conversion (IC), facilitated by non-adiabatic couplings (NACs) [42–47]. We note that the latter process is enabled by configuration interactions with charge-transfer configurations [44,46,47] and is similar to singlet fission [48,49], a process of generating two triplet excitons from a single singlet exciton.

In this contribution, we report high-level electronic structure calculations using QM/MM approach [50,51]. We consider protein-bound flavin chromophore, RF, with and without nearby oxygen molecule (about 4.1–4.2 Å away from RF). Our calculations provide quantitative support to earlier mechanistic proposals [42–44] put forward when computational power was not sufficient to carry out accurate *ab initio* calculations on realistic systems. Our results provide complimentary details to a large body of research on singlet oxygen generation by flavin-based systems.

2. Computational details

Our model structure was prepared in an earlier study [52], where it was constructed using crystal structure of miniSOG with the RF cofactor (PDB ID 7QF4) [8]. Hydrogen atoms were added assuming the conventional protonation states of the polar residues at neutral pH: Arg and Lys were charged positively, Glu and Asp were charged negatively and His85 was neutral. Following notations from Ref. [52], we refer to this model miniSOG[RF]. The initial structure was solvated and neutralised following the standard protocols, and ten dioxygen molecules were added to it at random places. The structure was then equilibrated using molecular dynamics with CHARMM36 forcefield topology and parameters [53], TIP3P water, and RF parameters in the oxidised form of flavin from Ref. [54]; for details, see Ref. [52]. Selected snapshots from equilibrium trajectories were optimised using QM/MM with the PBE0-D3 functional [55,56] and the 6–31G* basis set, and using the AMBER99 forcefield [57] for the MM part. Our model structure corresponds to the snapshot with the shortest oxygen-RF distance (about 4.1–4.2 Å).

The QM system included RF, O₂, sidechains of Gln77, Asn72, and Asn82, and seven water molecules. This structure – called model A – was also used to compute electronic states and relevant couplings. The structure is shown in Figure 2; the Cartesian coordinates were deposited on Zenodo (see the SI for details).

We carried out excited-state calculations using several structures derived from model A: (i) model A, (ii) model A without oxygen molecule (model B) and (iii) model B with oxygen molecule placed far away from the chromophore (~6–8 Å).

The excited states were computed using several approaches: TD-DFT (time-dependent density functional theory), RAS-CI (restricted active space configuration interaction) [58], and extended multiconfigurational quasi-degenerate perturbation theory of the second order (XMCQDPT2) [59]. The XMCQDPT2 calculations for model B were based on state-averaged CASSCF(10/8)/cc-pVDZ wavefunctions (14 states were used in the averaging). The XMCQDPT2 calculations for model A were based on state-averaged CASSCF(12/10)/cc-pVDZ wavefunctions (19 states were used in the averaging). We used Intruder State Avoidance shift of 0.02 hartree. We used default parameters for resolvent-fitting approximations. Active-space orbitals are shown in the SI. Because in XMCQDPT2 singlets and triplets are computed separately, the relative total energies of different multiplicity manifolds are not balanced. To correct for this mismatch, we shift the singlet manifold of the combined RF-O₂ system so that the excitation energy of the lowest state in the singlet manifold, which corresponds to the RF(S₀) × O₂(¹Δ_g) state, equals experimental [60] excitation energy of the O₂(³Σ_g⁻) → O₂(¹Δ_g) transition (0.97 eV).

We carried out SOC calculations using RASCI and TD-DFT. TD-DFT calculations are suitable for computing singlet and triplet excited states of closed-shell molecules, such as RF and FMN. However, electronic degeneracies in oxygen impart open-shell character [61] to the wave-functions of relevant states. Such states can be tackled either by multi-reference methods, such as CASSCF, or by spin-flip approaches [62,63]. As we explain below, the RF-O₂ system can be described by a double spin-flip approach, in the same fashion as was done before in the context singlet fission [64–66]. The RAS-2SF calculations have employed quintet reference corresponding to the high-spin RF(T₁) × O₂(³Σ_g⁻) restricted open-shell Hartree–Fock determinant.

The SOCs were computed as matrix elements of the spin–orbit part of the Breit–Pauli Hamiltonian. Two-electron contributions were computed using the mean-field approach [67–70].

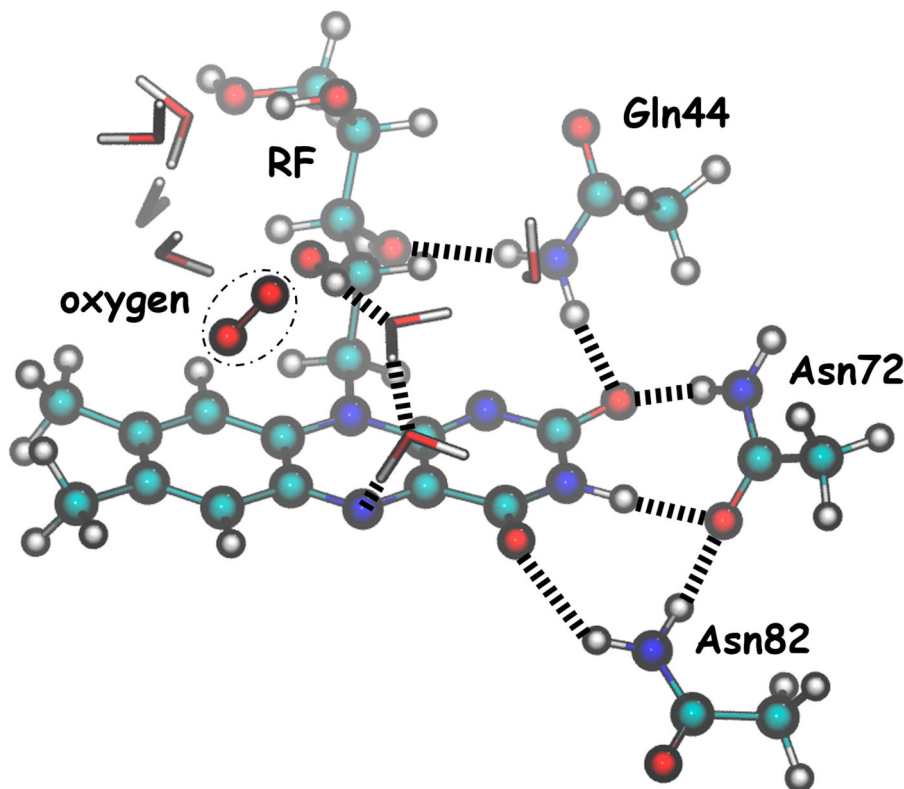


Figure 2. QM cluster (model system A) used for QM/MM optimisation and excited-state calculations: RF, O₂, sidechains of Gln77, Asn72, Asn82, and seven water molecules. Oxygen is located about 4.1–4.2 Å from RF.

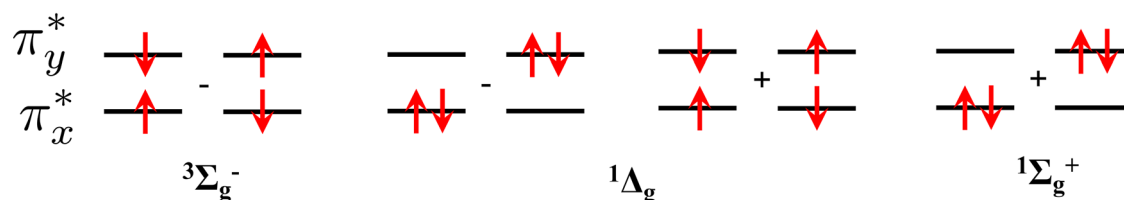


Figure 3. Electronic configurations of the $^3\Sigma_g^-$, $^1\Delta_g$ and $^1\Sigma_g^+$ states of molecular oxygen.

TD-DFT and RAS-CI calculations were carried out using the Q-Chem electronic structure package [71,72]. XMCQDPT2 calculations were carried out using Firefly [73].

3. Results and discussion

We begin by reviewing the basic energetics of the RF chromophore and molecular oxygen. Molecular oxygen's ground state is $^3\Sigma_g^-$. The next two states are singlets: doubly degenerate $^1\Delta_g$ and $^1\Sigma_g^+$ states located at 0.97 and 1.63 eV, respectively [38,60]. The electronic configurations of these four states can be described by distributing two electrons in two degenerate π^* orbitals – they are shown in Figure 3. There are four determinants – two of an open-shell type (in which the two π^* orbitals are singly occupied) and two of a closed-shell type (in which

one of the orbitals is doubly occupied and the second is empty). According to El-Sayed's rules [74], one can anticipate small (or zero) SOC between the determinants of the same type and large SOC between the closed-shell and open-shell determinants – since these are related by a transition between π_x^* and π_y^* and thus involve an orbital flip. To understand the SOC between these states, recall that each state is described by two determinants, so the combined effect depends on the relative signs (a similar situation was described in Ref. [75]). By analysing the configurations in Figure 3, one can see that the SOC between the $^3\Sigma_g^-$ and $^1\Delta_g$ is expected to be small (contributions from the two determinants cancel out) whereas the SOC between the $^3\Sigma_g^-$ and $^1\Sigma_g^+$ can be large (contributions from open-shell–closed-shell transitions add up). The calculation of SOC confirms this – at the RAS-SF/6-311G(d,p) level of theory, the respective SOC are 0.00 and 173.36 cm^{-1} .

Table 1. Excitation energies (eV) for model system B (no oxygen).

State	ω B97M-V/aug-cc-pVTZ	XMCQDPT2/cc-pVDZ ^a
S ₁	3.26 (0.33)	2.93 (0.42)
S ₂	3.84 (0.02)	3.60 (0.20)
T ₁	2.16	2.48
T ₂	2.82	2.96
T ₃	3.41	3.19

^aXMCQDPT2 is based on SA14-CASSCF(10/8) wavefunctions. The XMCQDPT2 calculations were carried out for a model structure with oxygen molecule ~ 8 Å away from RF (see text for details).

Oscillator strengths for the transitions from RF(S₀) are given in parenthesis.

Table 1 lists energies of the RF chromophore in the model miniSOG[RF] system; additional results are given in the SI. The computed energetics is similar to other flavin-based systems [37]: at the XMCQDPT2 level, the lowest triplet state is ~ 0.3 eV below S₁, and the second triplet is slightly above S₁. The S₂ state is ~ 0.7 eV above S₂. TD-DFT slightly overestimates excitation energy of the singlet and underestimates energies of the triplets relative to XMCQDPT2, however, the overall picture is similar. The RAS-SF singlet energies (shown in the SI) are overestimated due to the insufficient treatment of dynamical correlation).

Figure 4 shows NTOs for the S₀ \rightarrow T₁ and S₀ \rightarrow S₁ transitions in RF (model system B). The shape of NTOs is similar, consistent with the $\pi \rightarrow \pi^*$ character of the transitions. Because the two states have similar orbital character, the S₁ – T₁ SOC is expected to be small by virtue of El-Sayed's rules [74], as confirmed by the calculations – e.g. at the TD-DFT level, the S₁ – T₁ SOC is 0.58 cm⁻¹ (see the SI).

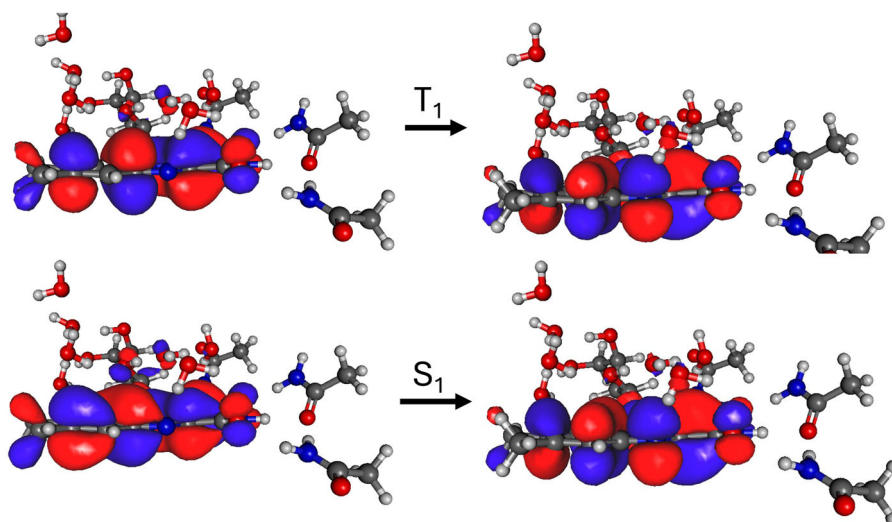
Such small values of S₀ \rightarrow T₁ SOC in flavin-based systems have been reported by previous studies [34,37]. They might appear puzzling in view of a high quantum efficiency of triplet-state yields [10,76] – as high as

0.4–0.5. Such efficient ISC in flavins is facilitated by spin-vibronic interactions, which entail contributions from higher triplet states [37,77,78] as well as enhancement of SOC upon bending motions of the chromophore. As we illustrate below, the production of triplet RF can be also enhanced by molecular oxygen via IC, as was observed experimentally [38,41–43] and explained theoretically [46,47].

To investigate possible pathways of the singlet oxygen production, we consider a model system that comprises the RF chromophore and a nearby oxygen molecule, embedded in the protein (model system A, see Computational Details). The low-lying electronic states of the combined RF-O₂ system can be described as products of $\Psi(\text{RF}) \times \Psi(\text{O}_2)$, and their energies can be estimated as a sum of the respective energies of the two moieties. We note that electronic configurations of these composite states are derived by distributing four electrons in the four orbitals – π and π^* orbitals of RF and two π^* orbitals of oxygen, a situation suitable for double spin-flip approach using a high-spin quintet reference (see Figure 5) [63,79].

Figure 6 shows energy diagram for the singlet and triplet manifolds obtained by combining energies of the isolated O₂ and RF (taken from model system B) using experimental energies for O₂ and our best estimates for the RF chromophore (XMCQDPT2 results). We note that a similar energy diagram was invoked by Tsubomura and Mulliken in 1960 [42] and by Minaev in 1985 [44].

Table 2 shows the results of XMCQDPT2 calculations for system A – as one can see, the differences between idealised estimates and the calculations are very small. Overall, the presence of O₂ has a negligible effect on the states' energies, as expected for this weakly interacting

**Figure 4.** NTOs for the two lowest transitions in RF cofactor in miniSOG[RF].

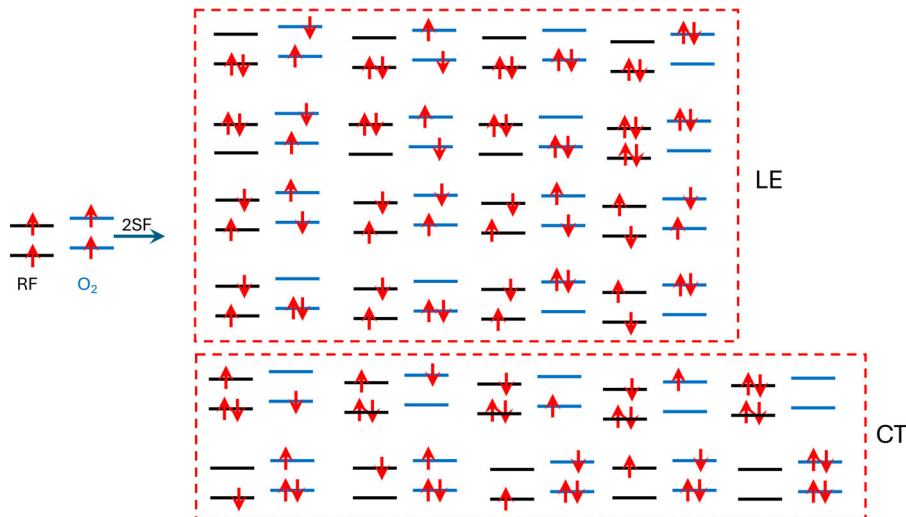


Figure 5. RAS-2SF reference and target determinants. Singly occupied orbitals are flavin’s π and π^* and oxygen’s π_x^* and π_y^* . LE and CT denote local excitations and charge-transfer configurations, respectively.

complex; thus, the energy diagram in Figure 6 provides a good description of energy levels. The RAS-2SF results are given in the SI. The RAS-2SF energies are less accurate than XMCQDPT2 due to an insufficient description of dynamic correlation. Inclusion of hp (hole-particle) excitations improves the energies significantly, but the changes in the wavefunctions and, consequently, the properties are small.

As one can see, upon excitation to the S_1 state of RF, several pathways for electronic relaxation are energetically possible in the triplet and singlet manifolds. The accessible states are: $\text{RF}(T_1) \times \text{O}_2(^3\Sigma_g^-)$, $\text{RF}(S_0) \times \text{O}_2(^1\Sigma_g^+)$ and $\text{RF}(S_0) \times \text{O}_2(^1\Delta_g)$.

To further analyse these pathways, we consider relevant electronic couplings – SOC between the states of

different multiplicity and NACs between the states of the same multiplicity. As a proxy for NAC, we consider the norm of one-particle transition density matrix, $\|\gamma\|$, between the two states [64,80] (large $\|\gamma\|$ signifies considerable one-electron character of the transition, which can develop due to the admixture of charge-transfer configurations). Figure 7 shows the computed couplings. First, we consider the initially excited state, $\text{RF}(S_1) \times \text{O}_2(^3\Sigma_g^-)$ (its multiplicity is triplet because of oxygen). The value of SOC that couples this state to the singlet state $\text{RF}(T_1) \times \text{O}_2(^3\Sigma_g^-)$ is small (0.07 cm^{-1}), as expected from the SOC value for the $T_1 - S_1$ coupling in RF. The value of SOC with the $\text{RF}(S_0) \times \text{O}_2(^1\Delta_g)$ states is larger (0.16 cm^{-1}). Thus, a single-step electronic transition producing $\text{O}_2(^1\Delta_g)$ is possible, but does not appear to be very effective. We note that the values of SOC can be significantly enhanced when oxygen is closer to the chromophore, as shown by Minaev and coworkers [46,47]. Hence, thermal fluctuations or structural relaxation of the excited-state collision complex can increase the yield. Importantly, the initially excited state shows a substantial NAC with *triplet* $\text{RF}(T_1) \times \text{O}_2(^3\Sigma_g^-)$, suggesting that this non-adiabatic transition may be fast and effective. This means that the production of triplet RF can proceed both via ISC and via IC, when oxygen is present. Such an oxygen-assisted pathway for the triplet production has been put forward by Tsubomura and Mulliken in 1960 [42] to explain enhanced ISC – an increased yield of triplet states in the presence of oxygen – first discussed by Kasha in 1950 [81]. This enhancement was also documented by Minaev and co-workers, who provided a theoretical support using semi-empirical calculations on a model system [44]. Tsubomura and Mulliken also posited

Table 2. Excitation energies (eV) for model system A; XMCQDPT2/cc-pVDZ^a.

State	Multiplicity	E_{ex} , eV
$\text{RF}(S_0) \times \text{O}_2(^3\Sigma_g^-)$	triplet	0.0
$\text{RF}(S_0) \times \text{O}_2(^1\Delta_g)$	singlet	0.97
$\text{RF}(S_0) \times \text{O}_2(^1\Delta_g)$	singlet	0.97
$\text{RF}(S_0) \times \text{O}_2(^1\Sigma_g^+)$	singlet	1.64
$\text{RF}(T_1) \times \text{O}_2(^3\Sigma_g^-)$	triplet	2.48
$\text{RF}(S_1) \times \text{O}_2(^3\Sigma_g^-)$	triplet	2.92 (0.422)
$\text{RF}(T_2) \times \text{O}_2(^3\Sigma_g^-)$	triplet	2.98
$\text{RF}(T_3) \times \text{O}_2(^3\Sigma_g^-)$	triplet	3.16
$\text{RF}(S_2) \times \text{O}_2(^3\Sigma_g^-)$	triplet	3.59 (0.204)
$\text{RF}(T_1) \times \text{O}_2(^1\Delta_g)$	triplet	3.60
$\text{RF}(T_1) \times \text{O}_2(^1\Delta_g)$	triplet	3.60
$\text{RF}(S_1) \times \text{O}_2(^1\Delta_g)$	singlet	3.80
$\text{RF}(S_1) \times \text{O}_2(^1\Delta_g)$	singlet	3.80

^aXMCQDPT2 is based on SA19-CASSCF(12/10) wavefunctions (see text for details).

Oscillator strengths for the transitions from $\text{RF}(S_0)$ are given in parentheses.

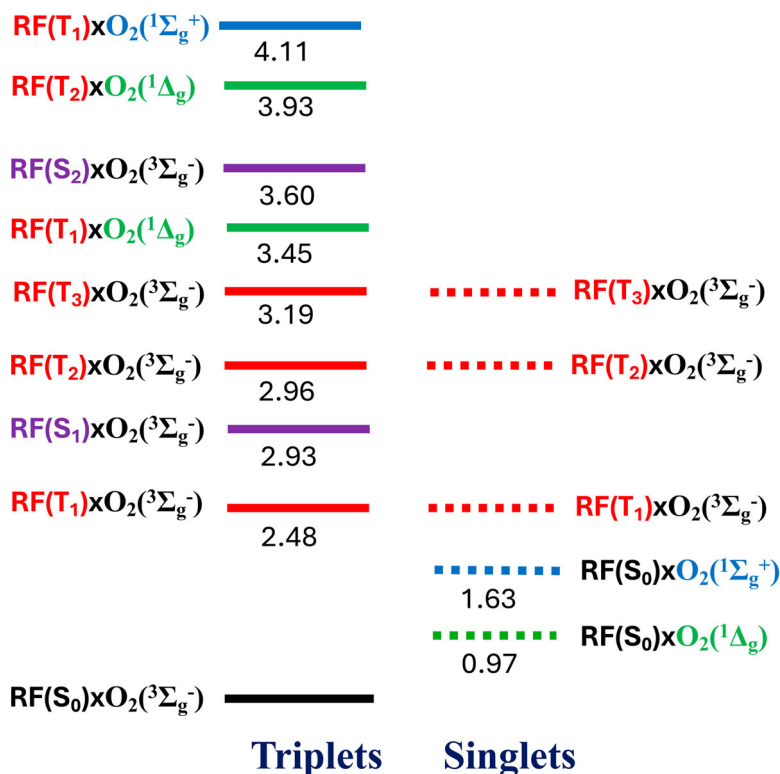


Figure 6. Energy diagram of the low-lying manifold of singlet and triplet states derived from RF's S_0 , S_1 , S_2 , T_1 , T_2 and T_3 and oxygen's $^3\Sigma_g^-$, $^1\Delta_g$ and $^1\Sigma_g^+$. Excitation energies are in electron-volt relative to the ground state, $\text{RF}(S_0) \times \text{O}_2(^3\Sigma_g^-)$.

that sufficiently large coupling between these states can develop via configuration interaction mixing of charge-transfer configurations [42], which was later illustrated by Minaev's calculations [44,46,47]. We note that the admixture of charge-transfer (or charge-resonance) configurations is also responsible for couplings facilitating singlet fission [64] and triplet-triplet annihilation [82,83].

We now consider possible transitions from the $\text{RF}(T_1) \times \text{O}_2(^3\Sigma_g^-)$ states. The singlet state of this character can be produced by either non-adiabatic transition described above or by a collision of oxygen molecule with the $\text{RF}(T_1)$ state formed by ISC. According to Figure 7, the singlet state of this character shows substantial NACs with lower states in the singlet manifold and, therefore, can lead to the singlet oxygen generation via IC. The triplet state of this character shows small but non-zero SOC with the $\text{RF}(S_0) \times \text{O}_2(^1\Sigma_g^+)$ and $\text{RF}(S_0) \times \text{O}_2(^1\Delta_g)$ (0.04 and 0.01 cm^{-1}). The reason why this state has small SOC with the lower states in the singlet manifold is because the respective transitions would involve changes of states of two electrons, which means that the only coupling terms can come from the exchange interaction, as in the Dexter energy transfer [84] or from the admixture of charge-transfer configurations. Again, both processes can be enhanced when oxygen is closer to the

chromophore, so for a quantitative description, sampling of the thermal motions and structural relaxation of the initially excited state are important.

We also note that involvement of higher states can both significantly increase the couplings and expand the available pathways. For example, upon excitation to S_2 , T_2 and T_3 become accessible. We also note that admixture of the $\text{RF}(T_1) \times \text{O}_2(^1\Sigma_g^+)$ state, which has large SOC (100 cm^{-1}) with $\text{RF}(T_1) \times \text{O}_2(^3\Sigma_g^-)$, can also contribute to the enhancement.

We note that some pathways lead to the production of $\text{O}_2(^1\Sigma_g^+)$. This other singlet oxygen has been observed experimentally [76]. It relaxes to $\text{O}_2(^1\Delta_g)$ with unit efficiency [76]. The computed value of the NAC for the $\text{RF}(S_0) \times \text{O}_2(^1\Sigma_g^+) \rightarrow \text{RF}(S_0) \times \text{O}_2(^1\Delta_g)$ transition is large, consistent with the experimental observations [76]. This large value suggests very fast internal conversion, which can outcompete ISC to the ground state of the system, $\text{RF}(S_0) \times \text{O}_2(^3\Sigma_g^-)$, which features rather large SOC (173 cm^{-1}).

Our results are consistent with previous mechanistic discussions of the singlet oxygen production and enhancement of radiative transitions due to collisions with other species [38,44,46,47,76]. The value of our contribution is that by providing concrete values of the electronic couplings it lands *ab initio* support to previously

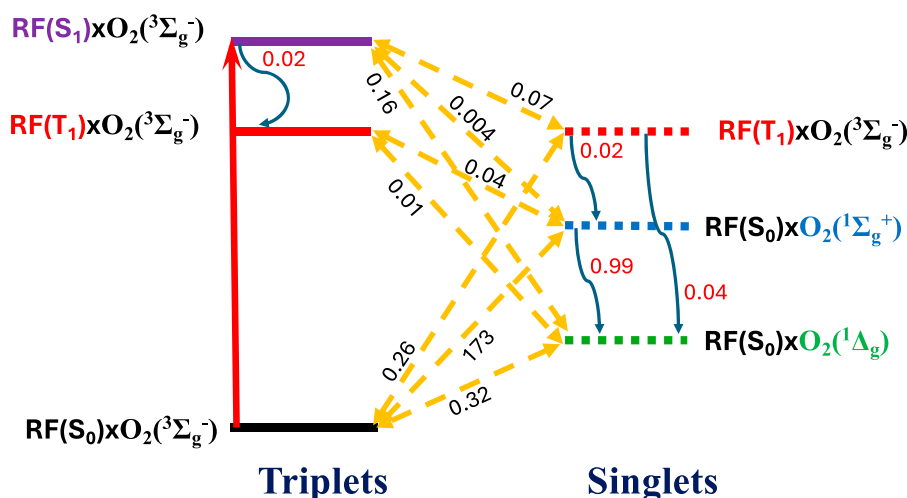


Figure 7. Couplings between the relevant states. SOC values (in cm^{-1}) are shown in black and $||\gamma||$ values (dimensionless) are shown in red. For the degenerate $^1\Delta_g$ states, the combined values (sum of the SOC/NACs for the two components) are shown.

hypothesised scenarios. We note that the pathway of singlet oxygen production via a *triplet* state of the oxygen-RF collision complex means that the kinetic models used to describe singlet oxygen production in flavin-based systems (such as one in Ref. [10]) need to be amended to account for different spin statistics.

4. Conclusion

We report high-level quantum chemistry calculations of a model system representing miniSOG photoactive protein with the RF chromophore. Our calculations of relevant electronic states and couplings between them clarify the mechanism of singlet oxygen generation in this system. In particular, our results indicate that singlet oxygen generation can proceed both via the singlet and the triplet $\text{RF}(T_1) \times \text{O}_2(^3\Sigma_g^-)$ state of the RF- O_2 complex. The triplet $\text{RF}(T_1) \times \text{O}_2(^3\Sigma_g^-)$ state can be produced either by IC of the initially excited S_1 state of RF bound to oxygen or by the T_1 state of RF (produced via ISC) forming a collision complex with O_2 . The relaxation of the singlet $\text{RF}(T_1) \times \text{O}_2(^3\Sigma_g^-)$ state proceeds via IC or Dexter energy transfer whereas the triplet $\text{RF}(T_1) \times \text{O}_2(^3\Sigma_g^-)$ state can decay via ISC facilitated by small but non-zero SOC. The couplings can be enhanced by sampling configurations in which oxygen is closer to the chromophore.

Our results provide robust theoretical support to previously hypothesised scenarios. We hope that a better understanding of the function of miniSOG will aid further development of effective genetically encoded photoactive proteins. Future work will focus on quantitative calculations of rates of the relevant processes and mechanisms of photodegradation and production of other types of ROS – such as peroxide – in these systems.

Acknowledgments

A.I.K. thanks Professor Boris Minaev from the Cherkasy National University for his valuable feedback on the manuscript.

Data availability statement

The data that support the findings of this study are available within the article and the associated SI.

Disclosure statement

The authors declare the following competing financial interest(s): A.I.K. is the president and a part-owner of Q-Chem, Inc.

Funding

We acknowledge support from the National Science Foundation (grant No. CHE-2154482 to A.I.K.) and resources of USC Advanced Research Computing (CARC) facilities. The Moscow team was supported by the Russian Science Foundation (project 22-13-00012). The research in Moscow was carried out using the equipment of the shared research facilities of HPC computing resources at the Lomonosov Moscow State University and supercomputer resources of the Joint Supercomputer Center of the Russian Academy of Sciences.

ORCID

Goran Giudetti  <http://orcid.org/0000-0003-3851-670X>

Bella L. Grigorenko  <http://orcid.org/0000-0003-1372-4692>

Anna I. Krylov  <http://orcid.org/0000-0001-6788-5016>

References

- [1] D.M. Chudakov, M.V. Matz, S. Lukyanov and K.A. Lukyanov, *Physiol. Rev.* **90**, 1103 (2010). doi:10.1152/physrev.00038.2009

- [2] A. Acharya, A.M. Bogdanov, K.B. Bravaya, B.L. Grigorenko, A.V. Nemukhin, K.A. Lukyanov and A.I. Krylov, *Chem. Rev.* **117**, 758 (2017). doi:10.1021/acs.chemrev.6b00238
- [3] C. Smith, *Nature* **492**, 293 (2012). doi:10.1038/492293a
- [4] D.L. Sai, J. Lee, D.L. Nguyen and Y.-P. Kim, *Exp. Mol. Med.* **53**, 495 (2021). doi:10.1038/s12276-021-00599-7
- [5] M.A. McLean, Z. Rajfur, Z. Chen, D. Humphrey, B. Yang, S.G. Sligar and K. Jacobson, *Anal. Chem.* **81**, 1755–1761 (2001). doi:10.1021/ac801663y
- [6] X. Shu, V. Lev-Ram, T.J. Deerinck, Y. Qi, E.B. Ramko, M.W. Davidson, Y. Jin, M.H. Ellisman and R.Y. Tsien, *PLoS Biol.* **9**, e1001041 (2011). doi:10.1371/journal.pbio.1001041
- [7] J. Torra, C. Lafaye, L. Signor, S. Aumonier, C. Flors, X. Shu, S. Nonell, G. Gotthard and A. Royant, *Sci. Rep.* **9**, 2428 (2019). doi:10.1038/s41598-019-38955-3
- [8] C. Lafaye, S. Aumonier, J. Torra, L. Signor, D. von Stetten, M. Noirclerc-Savoie, X. Shu, R. Ruiz-González, G. Gotthard, A. Royant and S. Nonell, *Photochem. Photobiol. Sci.* **21**, 1545 (2022). doi:10.1007/s43630-021-00156-1
- [9] M. Westberg, L. Holmegaard, F.M. Pimenta, M. Etzerodt and P.R. Ogilby, *J. Am. Chem. Soc.* **137**, 1632–1642 (2015). doi:10.1021/ja511940j
- [10] M. Westberg, M. Bregnhøj, M. Etzerodt and P.R. Ogilby, *J. Phys. Chem. B* **121**, 2561 (2017). doi:10.1021/acs.jpcc.7b00561
- [11] M. Westberg, M. Bregnhøj, M. Etzerodt and P.R. Ogilby, *J. Phys. Chem. B* **121**, 9366 (2017). doi:10.1021/acs.jpcc.7b07831
- [12] R. Ruiz-González, A.L. Cortajarena, S.H. Mejias, M. Agut, S. Nonell and C. Flors, *J. Am. Chem. Soc.* **135**, 9564 (2013). doi:10.1021/ja4020524
- [13] W. Holzer, J. Shirdel, P. Zirak, A. Penzkofer, P. Hegemann, R. Deutzmann and E. Hochmuth, *Chem. Phys.* **308**, 69 (2005). doi:10.1016/j.chemphys.2004.08.006
- [14] G. Strauss and W.J. Nickerson, *J. Am. Chem. Soc.* **83**, 3187 (1961). doi:10.1021/ja01476a005
- [15] P.F. Heelis, *Chem. Soc. Rev.* **11**, 15 (1982). doi:10.1039/cs9821100015
- [16] M. Insińska-Rak, A. Golczak and M. Sikorski, *J. Phys. Chem. A* **116**, 1199 (2012). doi:10.1021/jp2094593
- [17] W.M. Moore, J.T. Spence, F.A. Raymond and S.D. Colson, *J. Am. Chem. Soc.* **85**, 3367 (1963). doi:10.1021/ja00904a013
- [18] M. Halwer, *J. Am. Chem. Soc.* **73**, 4870 (1951). doi:10.1021/ja01154a118
- [19] M. Insińska-Rak, E. Sikorska, J.L. Bourdelande, I.V. Khmelinskii, W. Prukała, K. Dobek, J. Karolczak, I.F. Machado, L.F.V. Ferreira, E. Dulewicz, A. Komasa, D.R. Worrall, M. Kubicki and M. Sikorski, *J. Photochem. Photobiol. A* **186**, 14 (2007). doi:10.1016/j.jphotochem.2006.07.005
- [20] D.E. Metzler and W.L. Cairns, *J. Am. Chem. Soc.* **93**, 2772 (1971). doi:10.1021/ja00740a031
- [21] I. Ahmad and H.D.C. Rapson, *J. Pharm. Biomed. Anal.* **8**, 217 (1990). doi:10.1016/0731-7085(90)80029-O
- [22] M. Insińska-Rak, D. Prukała, A. Golczak, E. Fornal and M. Sikorski, *J. Photochem. Photobiol. A* **403**, 112837 (2020). doi:10.1016/j.jphotochem.2020.112837
- [23] M.A. Sheraz, S.H. Kazi, S. Ahmed, Z. Anwar and I. Ahmad, *Beilstein J. Org. Chem.* **10**, 1999–2012 (2014). doi:10.3762/bjoc.10.208
- [24] W.M. Moore and C. Baylor Jr., *J. Am. Chem. Soc.* **91**, 7170 (1969). doi:10.1021/ja01053a048
- [25] W. Holzer, A. Penzkofer, T. Susdorf, M. Álvarez, Sh. D.M. Islam and P. Hegemann, *Chem. Phys.* **302**, 105 (2004). doi:10.1016/j.chemphys.2004.03.017
- [26] W. Holzer, A. Penzkofer and P. Hegemann, *Chem. Phys.* **308**, 79 (2004). doi:10.1016/j.chemphys.2004.08.007
- [27] G.K. Radda and M. Calvin, *Biochemistry* **3**, 384–393 (1964). doi:10.1021/bi00891a014
- [28] B. Holmström, *Bull. Soc. Chim. Belges* **71**, 869 (1962). doi:10.1002/bscb.v71:11/12
- [29] P.-S. Song and D.E. Metzler, *Photochem. Photobiol.* **6**, 691 (1967). doi:10.1111/php.1967.6.issue-10
- [30] I. Ahmad, Q. Fasihullah, A. Noor, I.A. Ansari and Q.N.M. Ali, *Int. J. Pharm.* **280**, 199 (2004). doi:10.1016/j.ijpharm.2004.05.020
- [31] S. Salzmann, J. Tatchen and C.M. Marian, *J. Photochem. Photobiol. A* **198**, 221 (2008). doi:10.1016/j.jphotochem.2008.03.015
- [32] M.P. Kabir, Y. Orozco-Gonzalez and S. Gozem, *Phys. Chem. Chem. Phys.* **21**, 16526 (2019). doi:10.1039/C9CP02230A
- [33] M.P. Kabir, D. Ouedraogo, Y. Orozco-Gonzalez, G. Gadda and S. Gozem, *J. Phys. Chem. B* **127**, 1301 (2023). doi:10.1021/acs.jpcc.2c06475
- [34] K. Zenichowski, M. Gothe and P. Saalfrank, *J. Photochem. Photobiol. A* **190**, 290 (2007). doi:10.1016/j.jphotochem.2007.02.007
- [35] S. Salzmann, M.R. Silva-Junior, W. Thiel and C.M. Marian, *J. Phys. Chem. B* **113**, 15610 (2009). doi:10.1021/jp905599k
- [36] B.F. Minaev, H. Årgen and V.O. Minaeva, in *Spin–Orbit Coupling in Enzymatic Reactions and the Role of Spin in Biochemistry*, edited by J. Leszczynski (Springer, Dordrecht, 2016). pp. 1–31.
- [37] M. Bracker, M.K. Kubitz, C. Czekelius, C.M. Marian and M. Kleinschmidt, *ChemPhotoChem* **6**, e202200040 (2022). doi:10.1002/cptc.v6.7
- [38] P.R. Ogilby, *Chem. Soc. Rev.* **39**, 3181 (2010). doi:10.1039/b926014p
- [39] T. Förster, *Ann. Phys.* **2**, 55 (1948). doi:10.1002/andp.v437:1/2
- [40] D.L. Dexter, *J. Chem. Phys.* **21**, 836 (1953). doi:10.1063/1.1699044
- [41] H. Kautsky, *Trans. Faraday Soc.* **35**, 216 (1938). doi:10.1039/tf9393500216
- [42] H. Tsubomura and R.S. Mulliken, *J. Am. Chem. Soc.* **82**, 5966 (1960). doi:10.1021/ja01508a002
- [43] K. Kawaoka, A.U. Khan and D.R. Kearns, *J. Chem. Phys.* **46**, 1842 (1967). doi:10.1063/1.1840943
- [44] B.F. Minaev, *Zh. Prikl. Spektrosk.* **42**, 766 (1985). doi:10.1007/BF00661398.
- [45] B.F. Minaev, V.V. Bryukhanov, G.A. Ketsle, V. Ch. Laurinas, Z.M. Muldakhmetov, Zh. K. Smagulov and K.F. Regir, *Zh. Prikl. Spektrosk.* **50**, 291 (1989). doi:10.1007/BF00659989.
- [46] B.F. Minaev, S. Lunell and G.I. Kobzev, *Int. J. Quant. Chem.* **50**, 279 (1994). doi:10.1002/qua.v50:4

- [47] B.F. Minaev, V.V. Kukueva and H. Årgen, *J. Chem. Soc., Faraday Trans.* **90**, 1479 (1994). doi:10.1039/FT9949001479
- [48] M.B. Smith and J. Michl, *Annu. Rev. Phys. Chem.* **64**, 361 (2013). doi:10.1146/physchem.2013.64.issue-1
- [49] D. Casanova, *Chem. Rev.* **118**, 7164 (2018). doi:10.1021/acs.chemrev.7b00601
- [50] A. Warshel and M. Levitt, *J. Mol. Biol.* **103**, 227 (1976). doi:10.1016/0022-2836(76)90311-9
- [51] H.M. Senn and W. Thiel, *Angew. Chem. Int. Ed.* **48**, 1198 (2009). doi:10.1002/anie.v48:7
- [52] I. Polyakov, A. Kulakova and A.V. Nemukhin, *Biophysica* **3**, 252 (2023). doi:10.3390/biophysica3020016
- [53] R.B. Best, X. Zhu, J. Shim, P.E.M. Lopes, J. Mittal, M. Feig and A.D. MacKerell, *J. Chem. Theory Comput.* **8**, 3257 (2012). doi:10.1021/ct300400x
- [54] A. Alexandrov, *J. Comput. Chem.* **40**, 2834 (2019). doi:10.1002/jcc.v40.32
- [55] J.P. Perdew, K. Burke and M. Ernzerhof, *Phys. Rev. Lett.* **77**, 3865 (1996). doi:10.1103/PhysRevLett.77.3865
- [56] S. Grimme, J. Antony, S. Ehrlich and H. Krieg, *J. Chem. Phys.* **132**, 154104 (2010). doi:10.1063/1.3382344
- [57] J.W. Ponder and D.A. Case, *Adv. Prot. Chem.* **66**, 27 (2003).
- [58] D. Casanova and M. Head-Gordon, *Phys. Chem. Chem. Phys.* **11**, 9779 (2009). doi:10.1039/b911513g
- [59] A.A. Granovsky, *J. Chem. Phys.* **134**, 214113 (2011). doi:10.1063/1.3596699
- [60] G. Herzberg, *Molecular Spectra and Molecular Structure: I. Spectra of Diatomic Molecules*, Vol. I (van Nostrand Reinhold, New York, 1950).
- [61] A.I. Krylov, in *Reviews in Computational Chemistry*, edited by A.L. Parrill and K.B. Lipkowitz (Wiley, Hoboken, 2017), Vol. 30, pp. 151–224.
- [62] A.I. Krylov, *Chem. Phys. Lett.* **338**, 375 (2001). doi:10.1016/S0009-2614(01)00287-1
- [63] D. Casanova and A.I. Krylov, *Phys. Chem. Chem. Phys.* **22**, 4326 (2020). doi:10.1039/C9CP06507E
- [64] X. Feng, A.V. Luzanov and A.I. Krylov, *J. Phys. Chem. Lett.* **4**, 3845 (2013). doi:10.1021/jz402122m
- [65] X. Feng and A.I. Krylov, *Phys. Chem. Chem. Phys.* **18**, 7751 (2016). doi:10.1039/C6CP00177G
- [66] X. Feng, D. Casanova and A.I. Krylov, *J. Phys. Chem. C* **120**, 19070 (2016). doi:10.1021/acs.jpcc.6b07666
- [67] B.A. Hess, C.M. Marian, U. Wahlgren and O. Gropen, *Chem. Phys. Lett.* **251**, 365 (1996). doi:10.1016/0009-2614(96)00119-4
- [68] C.M. Marian, *WIREs: Comput. Mol. Sci.* **2**, 187 (2012).
- [69] P. Pokhilko, E. Epifanovsky and A.I. Krylov, *J. Chem. Phys.* **151**, 034106 (2019). doi:10.1063/1.5108762
- [70] A. Carreras, H. Jiang, P. Pokhilko, A.I. Krylov, P.M. Zimmerman and D. Casanova, *J. Chem. Phys.* **153**, 214107 (2020). doi:10.1063/5.0029146
- [71] A.I. Krylov and P.M.W. Gill, *WIREs: Comput. Mol. Sci.* **3**, 317 (2013).
- [72] E. Epifanovsky, A.T.B. Gilbert, X. Feng, J. Lee, Y. Mao, N. Mardirossian, P. Pokhilko, A.F. White, M.P. Coons, A.L. Dempwolff, Z. Gan, D. Hait, P.R. Horn, L.D. Jacobson, I. Kaliman, J. Kussmann, A.W. Lange, K.U. Lao, D.S. Levine, J. Liu, S.C. McKenzie, A.F. Morrison, K.D. Nanda, F. Plasser, D.R. Rehn, M.L. Vidal, Z.-Q. You, Y. Zhu, B. Alam, B.J. Albrecht, A. Aldossary, E. Alguire, J.H. Andersen, V. Athavale, D. Barton, K. Begam, A. Behn, N. Bellonzi, Y.A. Bernard, E.J. Berquist, H.G.A. Burton, A. Carreras, K. Carter-Fenk, R. Chakraborty, A.D. Chien, K.D. Closser, V. Cofer-Shabica, S. Dasgupta, M. de Wergifosse, J. Deng, M. Diedenhofen, H. Do, S. Ehlert, P.-T. Fang, S. Fatehi, Q. Feng, T. Friedhoff, J. Gayvert, Q. Ge, G. Gidofalvi, M. Goldey, J. Gomes, C.E. González-Espinoza, S. Gulania, A.O. Gunina, M.W.D. Hanson-Heine, P.H.P. Harbach, A. Hauser, M.F. Herbst, M. Hernández Vera, M. Hodecker, Z.C. Holden, S. Houck, X. Huang, K. Hui, B.C. Huynh, M. Ivanov, Á. Jász, H. Ji, H. Jiang, B. Kaduk, S. Kähler, K. Khistyayev, J. Kim, G. Kis, P. Klunzinger, Z. Koczor-Benda, J.H. Koh, D. Kosenkov, L. Koulias, T. Kowalczyk, C.M. Krauter, K. Kue, A. Kunitsa, T. Kus, I. Ladján-szki, A. Landau, K.V. Lawler, D. Lefrancois, S. Lehtola, R.R. Li, Y.-P. Li, J. Liang, M. Liebenthal, H.-H. Lin, Y.-S. Lin, F. Liu, K.-Y. Liu, M. Loipersberger, A. Luenser, A. Manjanath, P. Manohar, E. Mansoor, S.F. Manzer, S.-P. Mao, A.V. Marenich, T. Markovich, S. Mason, S.A. Maurer, P.F. McLaughlin, M.F.S.J. Menger, J.-M. Mewes, S.A. Mewes, P. Morgante, J.W. Mullinax, K.J. Oosterbaan, G. Parani, A.C. Paul, S.K. Paul, F. Pavošević, Z. Pei, S. Prager, E.I. Proynov, Á. Rák, E. Ramos-Cordoba, B. Rana, A.E. Rask, A. Rettig, R.M. Richard, F. Rob, E. Rossomme, T. Scheele, M. Scheurer, M. Schneider, N. Sergueev, S.M. Sharada, W. Skomorowski, D.W. Small, C.J. Stein, Y.-C. Su, E.J. Sundstrom, Z. Tao, J. Thirman, G.J. Tornai, T. Tsuchimochi, N.M. Tubman, S.P. Veccham, O. Vydrov, J. Wenzel, J. Witte, A. Yamada, K. Yao, S. Yeganeh, S.R. Yost, A. Zech, I.Y. Zhang, X. Zhang, Y. Zhang, D. Zuev, A. Aspuru-Guzik, A.T. Bell, N.A. Besley, K.B. Bravaya, B.R. Brooks, D. Casanova, J.-D. Chai, S. Coriani, C.J. Cramer, G. Cserey, A.E. DePrince, R.A. DiStasio, A. Dreuw, B.D. Dunietz, T.R. Furlani, W.A. Goddard, S. Hammes-Schiffer, T. Head-Gordon, W.J. Hehre, C.-P. Hsu, T.-C. Jagau, Y. Jung, A. Klamt, J. Kong, D.S. Lambrecht, W. Liang, N.J. Mayhall, C.W. McCurdy, J.B. Neaton, C. Ochsenfeld, J.A. Parkhill, R. Peverati, V.A. Rassolov, Y. Shao, L.V. Slipchenko, T. Stauch, R.P. Steele, J.E. Subotnik, A.J.W. Thom, A. Tkatchenko, D.G. Truhlar, T. Van Voorhis, T.A. Wesolowski, K.B. Whaley, H.L. Woodcock, P.M. Zimmerman, S. Faraji, P.M.W. Gill, M. Head-Gordon, J.M. Herbert and A.I. Krylov, *J. Chem. Phys.* **155**, 084801 (2021). doi:10.1063/5.0055522
- [73] A.A. Granovsky, *XMCQDPT2*, <http://classic.chem.msu.ru> (accessed Dec. 18, 2009).
- [74] M.A. El-Sayed, *Acc. Chem. Res.* **1**, 8 (1968). doi:10.1021/ar50001a002
- [75] M. Alessio, S. Kotaru, G. Giudetti and A.I. Krylov, *J. Phys. Chem. C* **127**, 3647 (2023). doi:10.1021/acs.jpcc.2c05940
- [76] M. Weldon, T.D. Poulsen, K.V. Mikkelsen and P.R. Ogilby, *Photochem. Photobiol.* **70**, 369 (1999). doi:10.1111/j.1751-1097.1999.tb08238.x
- [77] T.J. Penfold, E. Gindensperger, C. Daniel and C.M. Marian, *Chem. Rev.* **118**, 6975 (2018). doi:10.1021/acs.chemrev.7b00617
- [78] C. Marian, *Annu. Rev. Phys. Chem.* **72**, 617 (2021). doi:10.1146/physchem.2021.72.issue-1
- [79] D. Casanova, L.V. Slipchenko, A.I. Krylov and M. Head-Gordon, *J. Chem. Phys.* **130**, 044103 (2009). doi:10.1063/1.3066652

- [80] S. Matsika, X. Feng, A.V. Luzanov and A.I. Krylov, *J. Phys. Chem. A* **118**, 11943 (2014). doi:[10.1021/jp506090g](https://doi.org/10.1021/jp506090g)
- [81] M. Kasha, *Disc. Faraday Soc.* **9**, 14 (1950). doi:[10.1039/df9500900014](https://doi.org/10.1039/df9500900014)
- [82] B.F. Minaev, Theoretical model of triplet–triplet annihilation, *Izvestiya Vysshikh Uchebnykh Zavedenii, Fizika*, 12 (1977) [English version: Plenum Publishing Corporation, 0038-5697/78/2109-1120 (1979)].
- [83] M.J.Y. Tayebjee, D.R. McCamey and T.W. Schmidt, *J. Phys. Chem. Lett.* **6**, 2367 (2015). doi:[10.1021/acs.jpcllett.5b00716](https://doi.org/10.1021/acs.jpcllett.5b00716)
- [84] D.L. Dexter, *J. Lumin.* **18-19**, 779 (1979). doi:[10.1016/0022-2313\(79\)90235-7](https://doi.org/10.1016/0022-2313(79)90235-7)